Nanomaterial-incorporated blown bubble films for large-area, aligned nanostructures

Guihua Yu,[a] Xianglong Li,[b] Charles M. Lieber*[ac] and Anyuan Cao*[b]

Received 6th September 2007, Accepted 28th November 2007
First published as an Advance Article on the web 11th January 2008
DOI: 10.1039/b713697h

Developing flexible and scalable methods for controlled assembly of nanomaterials remains a critical challenge in nanotechnology. In this article, we review the progress in assembly of nanostructures with a focus on the recently reported method utilizing a bubble expansion process to align one-dimensional nanostructures embedded in blown bubble films. This approach is general and enables efficient assembly of a variety of nanomaterials over large areas on both rigid and flexible substrates, with good control on the orientation and density. The basic blown bubble film process, generality, mechanism, unique characteristics, and potential applications are discussed.

1. Introduction

Organized one-dimensional nanostructures such as nanowires and carbon nanotubes can possess unique physical properties that make them potential key building blocks for the manufacturing of next-generation high performance electronic, optoelectronic and electromechanical systems.[1–3] Yet, to realize such applications and to further fundamental studies of these materials will require development of effective methods for the assembly of nanowires (NWs) and nanotubes (NTs) with controlled location, orientation and spacing, hierarchically and over large areas.

To this end, much effort has been placed on developing methods of assembly of NWs and/or NTs.[4–23] For example, the Langmuir–Blodgett (LB) technique has been utilized to align NWs with controlled spacing and recently similar results have been achieved for single-walled nanotubes (SWNTs).[5–8] In the LB method, surfactant-wrapped NWs/SWNTs are slowly compressed on an aqueous subphase to yield uniaxially-aligned NWs/NTs. This technique produces parallel NWs/NTs with controlled spacing down to close-contact, and can be used to assemble more complex structures such as cross-bars by multiple layer transfer steps. Functional devices based on such LB films consisting of NWs or SWNTs have been fabricated,[7,8] although it is unclear whether the centimetre-square arrays of NWs can be scaled further to larger areas with high efficiency and transferred to non-rigid surfaces, such as flexible plastics.

Chemical modification of substrate surfaces has also been widely used to assemble NWs and SWNTs.[9–13] In this approach, chemically-patterned substrates are dipped into a nanomaterial-containing solution during which NWs or SWNTs adsorb onto the complementary patterned regions of the substrate. This method shows promise for assembly of nanostructure arrays at predetermined locations (determined by the chemical pattern), orientation, and pattern shape or hierarchy, although larger size patterns (*e.g.* on the order of several μm) of SWNTs exhibit

[a]*Department of Chemistry and Chemical Biology, Harvard University, Cambridge, Massachusetts 02138, USA. E-mail: cml@cmliris.harvard.edu; Fax: +1-617-496-5442; Tel: +1-617-496-3169*
[b]*Department of Mechanical Engineering, University of Hawaii at Manoa, Honolulu, Hawaii 96822, USA. E-mail: anyuan@hawaii.edu; Fax: +1-808-956-2373; Tel: +1-808-956-7597*
[c]*School of Engineering and Applied Sciences, Harvard University, Cambridge, Massachusetts 02138, USA*

Charles M. Lieber

Charles M. Lieber is the Mark Hyman Professor in the Department of Chemistry and Chemical Biology at Harvard University. Lieber is an elected member of the National Academy of Sciences and the American Academy of Arts and Sciences. He is one of the leading scientists in the field of nanoscience and nanotechnology with over 290 published papers and more than 30 patents. More details: http://cmliris.harvard.edu/people/CML.php.

Anyuan Cao

Anyuan Cao is an Assistant Professor in the Department of Mechanical Engineering at University of Hawaii at Manoa. He received his PhD in Mechanical Engineering from Tsinghua University, China, in 2002. He then moved to the US to pursue nanomaterials post-doctoral research under the guidance of Pulickel Ajayan. His research interests are in nanocomposites, nanomechanics, and energy related applications.

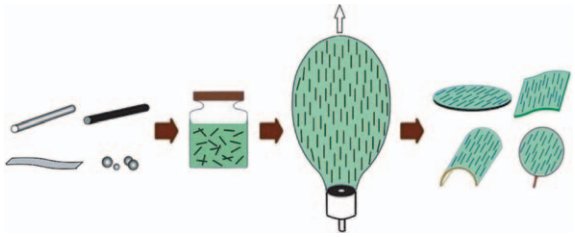

Fig. 1 Blown bubble film (BBF) approach. Nanomaterials (*e.g.* nanotubes, nanowires, nanobelts, and nanoparticles) are dispersed in a polymer solution, a volume of solution is expanded as a bubble using a die, and then BBFs are transferred to substrates, including crystalline wafers, plastic sheets, curved surfaces, and open frames. The black straight lines illustrated in the solution and bubble films represent one-dimensional nanomaterials such as nanowires or nanotubes.

reduced alignment.[10] Additional assembly methods have used liquid crystalline processing of NT solutions,[15] liquid or gas flow-channels,[16,17] external electrical or magnetic fields,[18,19] dielectrophoresis,[20] and contact printing of a NW directly from growth wafers,[21] to align NWs and NTs. In addition, DNA has been used in a templating process.[22,23] These processes either result in localized alignment[15] or require lithographic patterning of substrate and applied fields to achieve alignment.[18–20] Despite the many methods reported, it remains an open question whether they will enable assembly to be scaled from present centimetre regime to large wafers, which represents a scale important to many proposed electronic and photonic applications, and even areas as large as the metre scale, which open up unique opportunities in large-area displays and photovoltaics.

2. The blown bubble film approach

Every year several billion pounds of polymers are processed into plastic products (*e.g.* bags, films) by the blown film extrusion technique.[24–26] The commercial process involves continuous expansion of a polymer melt through a die as a bubble which is then processed as a continuous film. We have adapted the basic ideas underlying this commercial film production method to make thin films containing well-organized nanostructures. This approach for assembly of large area films of nanomaterial, which we term the blown bubble film (BBF) approach,[27] represents a very general platform technique for nanotechnology and may enable many applications. Our basic approach involves the preparation of a homogeneous solution containing dispersed nanomaterials, which is analogous to the polymer melt used in industry, expansion of a bubble from the nanomaterial solution at a controlled direction and speed, and then transfer of the bubble to substrates to yield well-defined nanomaterial-incorporated thin films (Fig. 1).

The BBF approach for assembling nanostructures has several distinct advantages compared with other methods described briefly above. First, this approach is general and can be used for organizing a wide range of nanoscale materials, including electronically and optically active NWs, multi-walled NTs (MWNTs) and SWNTs,[27] and in principle could be used to assemble nanobelts, graphene sheets, nanoparticles, and even heterojunctions (Fig. 1).[28–33] Second, this approach is highly scalable with the potential to achieve at least metre-scale dimensions based on results for pure films.[24] We have demonstrated bubbles with diameters over 30 centimetres using epoxy and a 50 mm die,[27] and larger bubbles should be possible by further optimizing the materials and process. Third, this approach yields ordered nanostructures in thin films that are robust as freestanding films, and that can be transferred to rigid, flexible and curved substrates

The nanomaterial-embedded bubble films can be considered as thin film nanocomposites. Conventional methods for preparing nanocomposite sheets or films include hot-pressing, solution casting, and spin-coating.[29,34–37] These methods are useful for small-scale sample testing, but are difficult to extend to large area films or continuous processing. In addition, the composites made by these methods typically contain randomly oriented nanomaterials, although alignment of nanostructures is critical to the development of many applications in electronics and photonics. In contrast, the blown bubble films reviewed in this article, which represent the first example of this technique being applied to nanocomposites, contain assembled nanostructures with uniform orientation and controlled density.

2.1 Nanomaterial solutions and bubble expansion

A homogeneous solution consisting of a specific nanomaterial uniformly dispersed in epoxy resin was prepared by functionalization of the nanomaterial surface and then mixing with epoxy. For example, purified SWNTs (Carbon Solutions, Inc.) were functionalized with octadecylamine (ODA),[38] and then a known mass of the ODA–SWNTs dispersed in tetrahydrofuran (THF) was transferred to a known mass of epoxy resin (Fig. 2a), and then mixed until homogeneous. The mixture was stirred to achieve a uniform solution, and hardener was added, and the mixture was capped and allowed to cure (*i.e.*, polymerize) until the viscosity increased to a range, 15–25 Pa s, suitable for

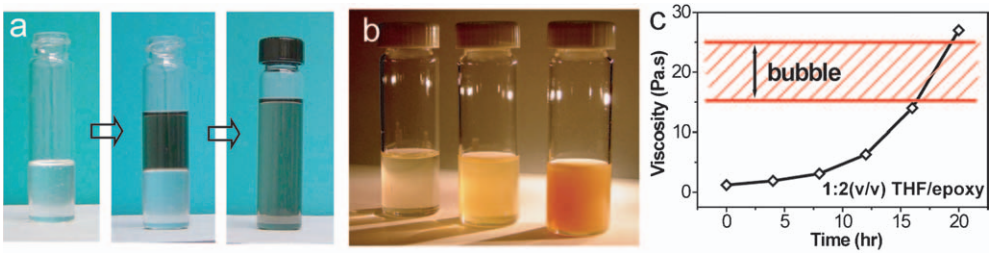

Fig. 2 Bubble solution preparation. (a) Mixing of NTs dispersed in THF with epoxy to make a uniform solution. (b) Different concentration SiNW–epoxy solutions: From left to right are 0.01, 0.03, 0.15 wt%, respectively. (c) Viscosity *versus* curing time for an epoxy solution, where the range suitable for bubble expansion is highlighted (hatched area).

producing stable bubbles. A similar method was used to prepare homogeneous SiNW–epoxy solutions except that 5,6-epoxyhexyltriethoxysilane was used to functionalize the surface of the SiNWs (Fig. 2b). A homogeneous solution, which can be aided by appropriate nanostructure surface functionalization, is important for uniform distribution of nanomaterials in the resulting bubble films.

The viscosity, which is determined by epoxy curing time, is a key parameter that determines the best stage for blowing bubbles. The desired viscosity range for blowing large bubbles is 15 to 25 Pa s (Fig. 2c). Bubbles break easily when blowing at higher viscosity and only small bead-like bubbles could be blown at lower viscosity. Addition of THF to the nanostructure–epoxy solution is important for two reasons. First, the solvent helps disperse nanomaterials, and second, it prolongs the cross-linking process. The latter is important for achieving stable viscosity for bubble expansion, and in the absence of THF we were unable to produce bubbles by this overall approach.

Controlled bubble initiation, expansion, and transfer were done using a 50 mm diameter circular die with a gas inlet at the bottom and outlet at the top surface (Fig. 3a). The nanomaterial–epoxy solution was deposited on the die surface and blown into a bubble by flowing gas at a pressure of 150 to 200 kPa (Fig. 3b–d). The upward bubble expansion was stabilized and controlled by a motor-driven ring. Bubbles were expanded in an elongated spherical shape (along the vertical axis), and sample substrates, such as silicon wafers, were fixed close to the central region of the elongated bubble during the transfer process. Samples transferred from top or bottom regions of the bubble, will yield varying alignment direction across the substrate surface. Typically, bubbles were expanded upwards at a speed of about 15 cm min^{-1} until the outer surface of the bubble conformally coated silicon wafers (Fig. 3d) or other substrates. Bubbles with diameters of >30 centimetres have been blown from about 0.5 g nanostructure–epoxy solution and transferred conformally to 150 mm wafers. The wafers with BBF coatings were characterized by optical and electron microscopy to determine the distribution and orientation of nanomaterials.

2.2 Control of nanomaterial alignment and density

SiNW-BBFs were transferred to 150 mm diameter wafers to characterize the distribution and orientation of the NWs within the film. Representative dark-field optical images recorded from widely separated regions on a transferred BBF (Fig. 4a) show that the SiNWs have similar orientation and good alignment along the expansion direction of the bubble. The angular spread of the SiNWs is less than 10° over the entire 6 inch diameter substrate. In addition, excellent orientational alignment of the SiNWs within the BBFs over large areas is a general characteristic observed for all of the stable SiNW–epoxy solutions we have studied, with concentrations from 0.01 to 0.22 wt%.

We have characterized the density and separation of the aligned NWs in transferred films as a function of wt% solution

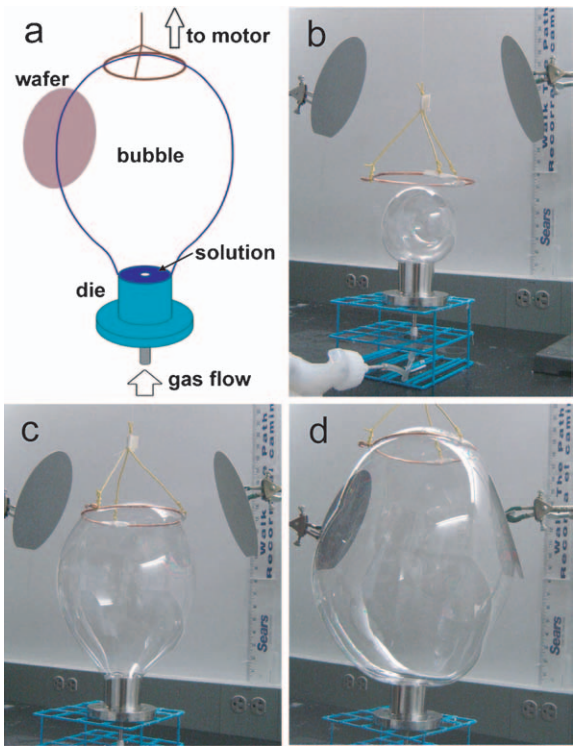

Fig. 3 Bubble expansion process. (a) Illustration of the apparatus including a 50 mm circular die with epoxy solution deposited on the top surface, and bubble expansion in gas flow directed upward using a ring connected to a motor. Wafers are fixed near the bubble for BBF transfer. (b), (c), (d) Snapshots of the initial, middle, and final stages of bubble expansion and coating of BBF on two 150 mm wafers.

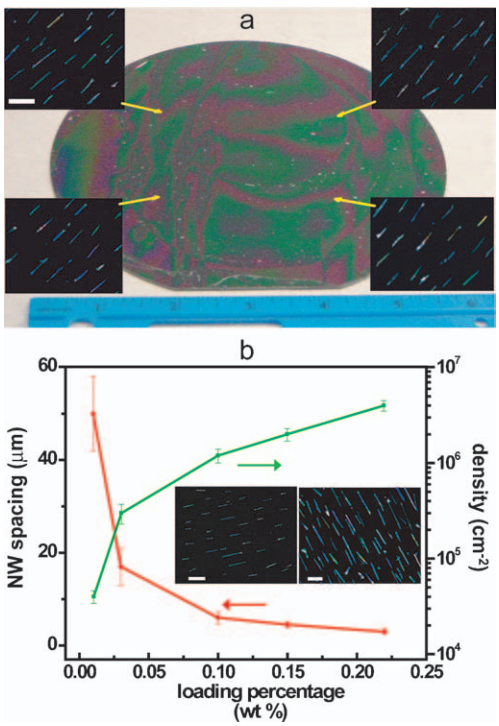

Fig. 4 Characterization of nanomaterial alignment and density. (a) Optical image of a 0.10 wt% SiNW-BBF on 150 mm Si wafer. Insets, dark-field (DF) optical images showing aligned SiNWs at different locations. Scale bar: 10 μm. (b) The NW spacing and density *versus* NW loading plot. Insets, two DF optical images taken from 0.03 and 0.15 wt% SiNW-BBFs. Scale bars: 20 μm (left), 10 μm (right). Adapted from Ref. 27.

used for bubble expansion, summarized in the plot (Fig. 4b). The transferred SiNW-BBFs show a clear decrease in NW separation and increase in density as the starting SiNW concentration increases from 0.01 to 0.22 wt%. We find that the NW separation can be systematically varied over an order of magnitude from 50 to 3.0 μm as concentration increases from 0.01 to 0.22 wt%, respectively; correspondingly NW density increases from 4.0×10^4 to 4.0×10^6 cm^{-2}. Compared with submicron spacing achieved by the LB technique, the NW spacing produced by the BBF approach is relatively modest, but it is still useful for applications such as nanoelectronic sensor arrays.[39] The spacing (density) *versus* wt% curves show some saturation at the higher SiNW concentrations. This tendency towards saturation is believed to be in part attributed to NW aggregation observed at higher concentrations. Further optimizing of the surface chemistry for the preparation of uniform higher wt% solutions would allow us to test the separation limits achievable with this approach and also to extend to different polymer systems besides epoxy, which offers great flexibility and compatibility with polymer industry.

2.3 Mechanism for alignment and drift of nanomaterials

The alignment of nanomaterials in bubble films has been attributed to the shear stress present in the epoxy fluid during the bubble expansion process,[40] particularly when the solution passes over the edge of the die (Fig. 5a). The shear strain rate at this point can be estimated by $\gamma = U_{fluid}/\delta \approx 5\ s^{-1}$, where U_{fluid} is the flow velocity close to the top surface of the fluid (~15 cm min^{-1}) and δ is the fluid depth at the edge (~0.5 mm). The corresponding shear stress is $\tau = \gamma\mu \approx 125$ Pa given a viscosity (μ) of 25 Pa s, which is responsible for aligning nanomaterials along the flow direction. The Peclet number (Pe) for the nanomaterial–epoxy system can be estimated by $Pe = L^3\gamma\mu/kT = 10^3$–$10^6$, where L is the NW/NT length (2–50 μm), and kT is the thermal energy.[41] The large value of Pe ($\gg 1$) indicates that the motion of nanomaterials during bubble expansion is dominated by hydrodynamic flow rather than diffusion.

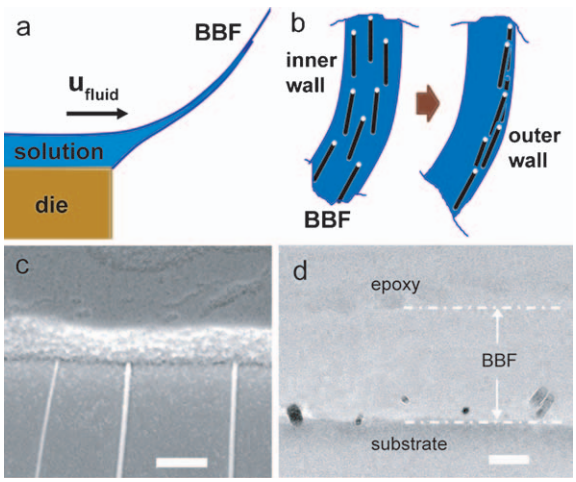

Fig. 5 Alignment of nanomaterials in BBFs. (a) Illustration of the bubble solution passing over the edge of the die at a speed of U_{fluid} during the expansion process. (b) Illustration of the migration of nanomaterials in the bubble film toward the outer wall of the bubble. (c) Cross-sectional SEM image of a SiNW-BBF showing three aligned NWs sitting close to the bottom of the film. Scale bar: 500 nm. (d) Cross-sectional TEM image showing that most of the NWs are located at the bottom of the film, thus near the substrate. Scale bar: 100 nm.

Another unique feature of BBFs is that the nanomaterials are located in approximately a single layer close to the outer surface of the bubble (Fig. 5b), as shown by the cross-sectional images of the scanning electron microscopy (SEM) and transmission electron microscopy (TEM) images (Fig. 5c,d). Since the initial solution contains uniformly dispersed nanomaterials, these results imply that the nanomaterials migrate to the outer bubble surface during expansion, as illustrated in Fig. 5b. The migration of nanomaterials has been attributed to the pressure gradient through the bubble film (the expansion pressure is ~150 kPa), and yields a driving force described by the Faxen Laws.[42] Specifically, the drift velocity of nanomaterials ($U_{NM} - U_{fluid}$) in fluid epoxy can be calculated as $U_{NM} - U_{fluid} = c^2\nabla^2 U_{fluid}/6 = (c^2/6\mu)(\partial p/\partial r)$, where U is the velocity along the normal direction (subscripts denote nanomaterials or fluid), c is the nanomaterial radius (10 to 20 nm), μ is viscosity (15–25 Pa s) and $\partial p/\partial r$ is the pressure gradient along the normal to the interface. Based on a pressure difference of 50 kPa at the inner and outer wall of the bubble, and a bubble thickness of 200–500 nm, this model predicts that the nanomaterials embedded will drift at a velocity on the order of 100 nm s^{-1}. Given that bubble expansion typically lasts for several seconds, the nanomaterials have sufficient time to move to the outer surface of the bubble film as observed experimentally.

2.4 BBFs containing different nanomaterials and polymers

BBFs containing other nanomaterials have been produced, including SWNTs (Fig. 6a), MWNTs (Fig. 6b), fluorescent cadmium sulfide (CdS) NWs (Fig. 6c), and nanoparticles. High aspect-ratio nanostructures (*e.g.* NWs and NTs) assembled in BBFs all exhibit a uniform distribution and a high degree of alignment, despite differences in material composition, diameter, length, and morphology. SWNT-BBFs were made by first functionalizing SWNTs with ODA, and then blowing bubbles from a SWNT-loaded epoxy solution. SEM examination shows that functionalized SWNT bundles have a diameter of 5 to 15 nm and length of 1 to 2 μm. Even with this short length, SWNTs are still highly aligned over large areas at an average separation of 1.5 μm and a density of about 5×10^7 cm^{-2} (Fig. 6a). Effective functionalization to achieve high solubility (>2 mg mL^{-1}) of SWNTs in THF was a key factor to prevent aggregation in these studies. A decrease in spacing and increase in density was also observed for the SWNT-BBFs as the SWNT solution concentration was increased.

MWNT-BBFs were made by a similar process as for SWNTs, and show good NT alignment as well (Fig. 6b). The MWNTs with length of >50 μm were initially curled in the bubble solution (inset, Fig. 6b), but became straight after bubble expansion. The straightening of MWNTs suggests that a strong shear force during bubble expansion may straighten the MWNTs. The uniformly spaced MWNTs and SWNTs in BBFs are distinct from many reported structures such as macroscopic mats and sheets containing random and entangled nanotubes,[43–45] and such uniform separation of NTs and other nanomaterials embedded in BBFs is desirable for making contacts and nanodevices based on individual nanostructures.

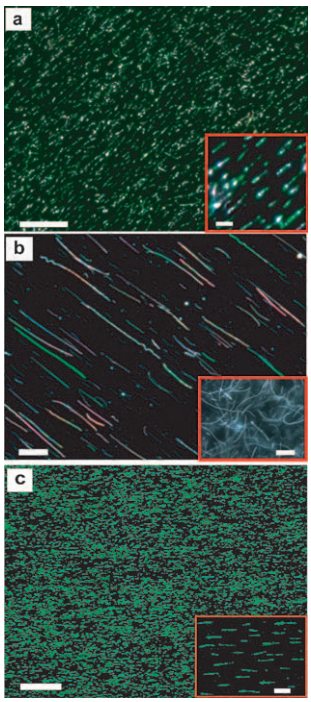

Fig. 6 BBFs containing different nanomaterials. (a) DF optical image of aligned SWNTs in a SWNT-BBF. Scale bar: 10 μm, and 2 μm (inset). (b) DF optical image taken from a MWNT-BBF showing aligned MWNTs. Scale bar: 20 μm. Inset, DF optical image showing curled MWNTs in solution before bubble expansion. Scale bar: 20 μm. (c) Confocal microscopy image of fluorescent CdS NWs embedded in a BBF. Scale bar: 50 μm, and 10 μm (inset). Adapted from Ref. 27.

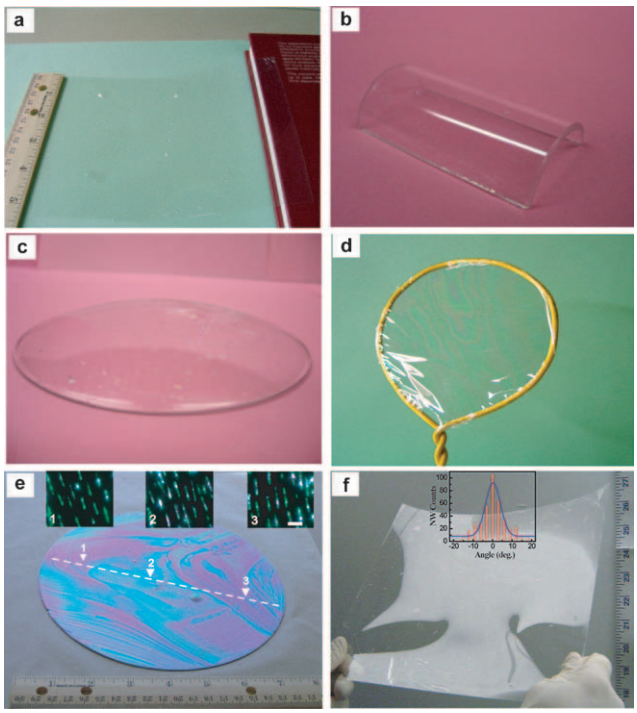

Fig. 7 BBFs transferred to different surfaces and very large substrates. The transferred surfaces include: (a) thin plastic sheet, (b) a half cylinder surface, (c) a curved watch glass, and (d) an open frame. (e) Optical image of a SWNT-BBF transferred to a 200 mm wafer with aligned SWNTs shown in insets. Scale bar: 2 μm. (f) Optical image of a SiNW-BBF transferred to a rectangular 9 inch × 12 inch flexible plastic sheet. Inset, histogram of angular distribution of NWs from different locations of the film. Adapted from Ref. 27.

Furthermore, confocal optical microscopy images of CdS NW-BBFs show that the CdS NWs were also uniformly distributed within the films.[27] As a last example, we have made nanoparticle-BBFs using 40 nm diameter SiC nanoparticles. Optical imaging shows individual or small aggregations of SiC nanoparticles at a distance of hundreds of nanometers to a few micrometers at an initial solution concentration of 0.1–0.6 wt%. Preliminary results suggest that the nanoparticles are uniformly distributed in BBFs and do not form more ordered structures such as one-dimensional chains (of nanoparticles). Bubbles with a size of >10 inches could be easily blown from high concentration nanoparticle solutions (*e.g.* >0.6 wt%), and BBFs containing uniformly distributed, high density individual nanoparticles are possible by appropriate functionalization to ensure homogeneous dispersion in the epoxy matrix. Taken together these results demonstrate a great materials diversity possible for nanomaterial-BBFs.

In addition, the blown bubble method can be extended to other polymer systems (*versus* epoxy). For example, poly(methyl methacrylate) (PMMA), a photoresist material for UV photolithography and electron-beam lithography, has been employed to make bubbles embedded with SiNWs or MWNTs, and these BBFs have been directly processed by photolithography to pattern nanoelectronic devices.[46]

2.5 BBF transfer and scale up

Another unique key feature of the BBF approach is that BBFs with aligned nanostructures can be transferred to a broad range of substrates with virtually any material composition or shape. For example, SiNW- and SWNT-BBFs were transferred directly to thin plastic sheets, a half-cylinder, a watch glass, and suspended across open frames as free-standing films (Fig. 7a–d), thus demonstrating much greater flexibility of this approach over other assembly approaches reported previously.

Our BBF approach also has the potential to be scaled to very large area structures, in analogy to large plastic films manufactured in industry.[24–26] As an initial demonstration of this point, we have successfully transferred SWNT-BBFs to 200 mm wafers (Fig. 7e), where the embedded SWNTs are uniformly aligned across the wafer surface, and transferred a SiNW-BBF to a rectangular 9 inch × 12 inch flexible plastic sheet (Fig. 7f) with good control of SiNW alignment and density across the entire flexible sheet. Both of these examples are the largest demonstrations to date for aligned NWs and NTs.

2.6 Application of BBFs: SiNW FET arrays

To demonstrate the potentially broad application of these nanomaterial-BBFs in electronics, large arrays of independently addressable NW FETs were fabricated using SiNW-BBFs transferred to 3 inch diameter flexible plastic substrates. This straightforward transfer of aligned SiNW-BBFs to large substrates makes this process considerably more efficient than previously reported fluid-directed[16] and Langmuir–Blodgett[6] assembly methods.

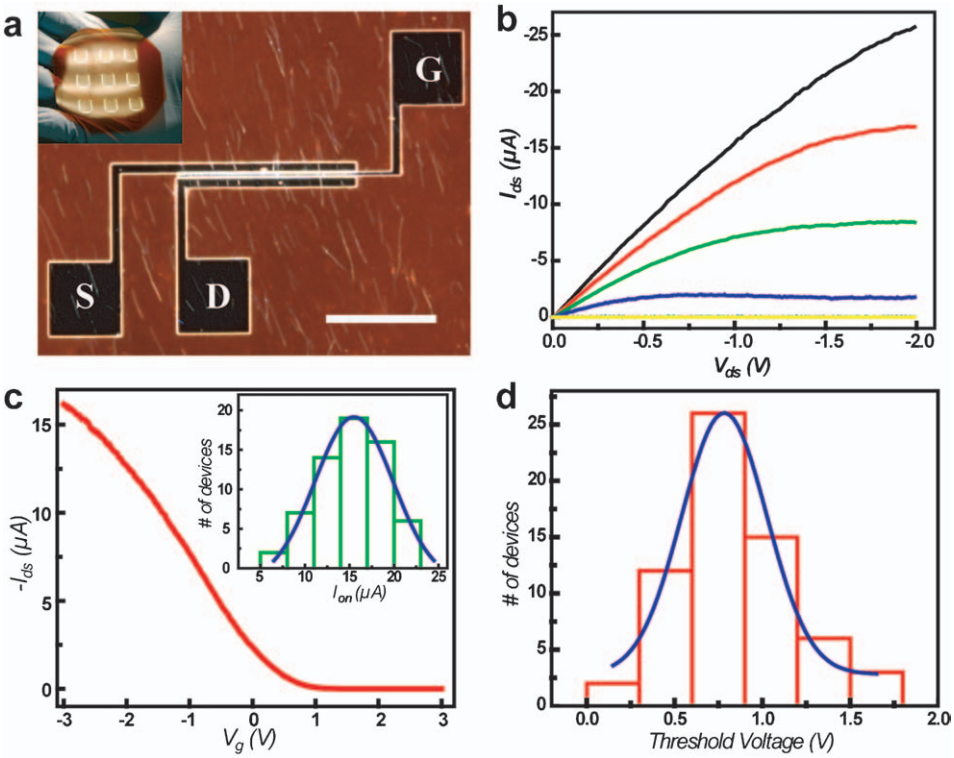

Fig. 8 SiNW transistor arrays fabricated on flexible plastics. (a) DF optical image of a top-gated multi-NW transistor device. Scale bar: 50 μm. Inset, photograph of a plastic substrate containing 3 × 3 NW FETs device arrays with each array containing 400 devices. (b) Typical I_{ds}–V_{ds} curves of a multi-NW FET. (V_g −3 V to 3 V, from top to bottom). (c) Typical I_{ds}–V_g characteristics with V_{ds} at −1 V. Inset, histogram of I_{on} showing uniform device characteristics. (d) Histogram of V_t from analysis of over 60 randomly chosen devices in the array. Adapted from Ref. 27.

Fig. 8a shows the device structure of top-gated multi-NW transistors. Representative output characteristics (Fig. 8b) show that the drain-source current (I_{ds}) first increases then saturates with increasingly negative drain voltage (V_{ds}) and that I_{ds} increases as the gate-voltage (V_g) decreases from 3 to −3 V; that is, characteristic of a p-type depletion mode FET. The I_{ds}–V_g transfer curve (Fig. 8c) yields the peak transconductance g_m of 6 μS, on current I_{on} of ~16 μA, on/off ratio >10^5, and threshold voltage V_t of 0.55 V. These key device characteristics compare well with multi-NW FETs prepared by the LB technique.[7] More importantly, histograms of the V_t and I_{on} (Fig. 8d; inset, Fig. 8c) demonstrate that these key FET properties are well-constrained and reproducible.

3. Conclusions and outlook

The BBF approach for assembling nanomaterials has been reviewed, and key features such as generality, alignment and density control, large area, and conformal transfer to various substrates have been outlined. Nanomaterial-BBFs with distinct nanomaterial properties, including metallic conduction, semiconductor properties, and optical emission, can serve as a powerful platform for manufacturing electrically and/or optically active films enabling many applications. Nanomaterial-BBFs prepared using other types of polymers that enable direct processing by photolithography and/or electron-beam lithography, such as PMMA, can facilitate device fabrication steps compared to the original epoxy polymer system. While there are scientific and engineering issues that should be tackled in the future, including (i) optimization of density, (ii) extension to other polymer systems, and (iii) a fundamental understanding of forces and dynamics during bubble expansion, we remain very optimistic about the potential of this approach for opening up applications and new scientific directions. For example, nanostructure-BBFs could be fabricated as reinforced nanocomposite films/coatings which have visible/infrared absorption and fluorescence,[47] NW/NT-BBFs could yield flexible nanoelectronic systems integrating high-performance FETs and chemical/biological sensors for environmental and medical applications,[39,48] and NW/NT-BBFs might lead to ultra-large area high-density, flat panel displays.[49] Moreover, by layering multiple nanostructure-BBFs or folding/scrolling nanomaterials-BBFs, more complex three-dimensional structures such as crossbars and hierarchically arranged nanoscale building blocks[21,50] might be fabricated to enable completely new types of electronic/photonic systems in the future.

Acknowledgements

A. Cao and C. M. Lieber acknowledge funding support from the US National Science Foundation (NSF) grant CMMI-0728197. C. M. Lieber also acknowledges support of the Air Force Office of Scientific Research and Samsung Electronics.

References

1 C. M. Lieber and Z. L. Wang, *MRS Bull.*, 2007, **32**, 99.
2 R. H. Baughman, A. A. Zakhidov and W. A. de Heer, *Science*, 2002, **297**, 787.
3 H. Dai, *Acc. Chem. Res.*, 2002, **35**, 1035.

4 Y. Yan, M. B. Chan-Park and Q. Zhang, *Small*, 2007, **3**, 24.
5 A. Tao, F. Kim, C. Hess, J. Goldberger, R. He, Y. Sun, Y. Xia and P. Yang, *Nano Lett.*, 2003, **3**, 1229.
6 D. Whang, S. Jin, Y. Wu and C. M. Lieber, *Nano Lett.*, 2003, **3**, 1255.
7 S. Jin, D. Whang, M. C. McAlpine, R. S. Friedman, Y. Wu and C. M. Lieber, *Nano Lett.*, 2004, **4**, 915.
8 X. Li, L. Zhang, X. Wang, I. Shimoyama, X. Sun, W.-S. Seo and H. Dai, *J. Am. Chem. Soc.*, 2007, **129**, 4890.
9 S. G. Rao, L. Huang, W. Setyawan and S. Hong, *Nature*, 2003, **425**, 36.
10 M. Lee, J. Im, B. Y. Lee, S. Myung, J. Kang, L. Huang, Y.-K. Kwon and S. Hong, *Nat. Nanotechnol.*, 2006, **1**, 66.
11 Y. Wang, D. Maspoch, S. Zou, G. C. Schatz, R. E. Smalley and C. A. Mirkin, *Proc. Natl. Acad. Sci. U. S. A.*, 2006, **103**, 2026.
12 H. Shimoda, S. J. Oh, H. Z. Geng, R. J. Walker, X. B. Zhang, L. E. McNeil and O. Zhou, *Adv. Mater.*, 2002, **24**, 899.
13 J. B. Hannon, A. Afzali, Ch. Klinke and Ph. Avouris, *Langmuir*, 2005, **21**, 8569.
14 B. S. Shim and N. A. Kotov, *Langmuir*, 2005, **21**, 9382.
15 H. Ko and V. V. Tsukruk, *Nano Lett.*, 2006, **6**, 1443.
16 Y. Huang, X. Duan, Q. Wei and C. M. Lieber, *Science*, 2001, **291**, 630.
17 H. Xin and A. T. Woolley, *Nano Lett.*, 2004, **4**, 1481.
18 P. A. Smith, C. D. Nordquist, T. N. Jackson and T. S. Mayer, *Appl. Phys. Lett.*, 2000, **77**, 1399.
19 D. P. Long, J. L. Lazorcik and R. Shashidhar, *Adv. Mater.*, 2004, **16**, 814.
20 A. Vijayaraghavan, S. Blatt, D. Weissenberger, M. Oron-Carl, F. Hennrich, D. Gerthsen, H. Hahn and R. Krupke, *Nano Lett.*, 2007, **7**, 1556.
21 A. Javey, S. W. Nam, R. S. Friedman, H. Yan and C. M. Lieber, *Nano Lett.*, 2007, **7**, 773.
22 K. Keren, R. S. Berman, E. Buchstab, U. Sivan and E. Braun, *Science*, 2003, **302**, 1380.
23 R. S. Mclean, X. Huang, C. Khripin, A. Jagota and M. Zheng, *Nano Lett.*, 2006, **6**, 55.
24 K. Cantor, *Blown Film Extrusion: An Introduction*, Hanser Gardner Publications, Cincinnati, 2006.
25 J. H. Briston, *Plastics Films*, Longman Scientific & Technical, UK, 1989, pp. 71–86.
26 W. R. R. Park, *Plastics Film Technology*, Robert E. Krieger Publishing Company, Huntington, New York, 1973.
27 G. Yu, A. Cao and C. M. Lieber, *Nat. Nanotechnol.*, 2007, **2**, 372.
28 Z. W. Pan, Z. R. Dai and Z. L. Wang, *Science*, 2001, **291**, 1947.
29 S. Stankovich, D. A. Dikin, G. H. B. Dommett, K. M. Kohlhaas, E. J. Zimney, E. A. Stach, R. D. Piner, S. T. Nguyen and R. S. Ruoff, *Nature*, 2006, **442**, 282.
30 Y. Xia, P. Yang, Y. Sun, Y. Wu, B. Mayers, B. Gates, Y. Yin, F. Kim and H. Yan, *Adv. Mater.*, 2003, **15**, 353.
31 M. S. Gudiksen, L. J. Lauhon, J. Wang, D. C. Smith and C. M. Lieber, *Nature*, 2002, **415**, 617.
32 L. J. Lauhon, M. S. Gudiksen, D. Wang and C. M. Lieber, *Nature*, 2002, **420**, 57.
33 J. Xiang, W. Lu, Y. Hu, Y. Wu, H. Yan and C. M. Lieber, *Nature*, 2006, **441**, 489.
34 N. Grossiord, J. Loos, O. Regev and C. E. Koning, *Chem. Mater.*, 2006, **18**, 1089.
35 B. E. Kilbride, J. N. Coleman, J. Fraysse, P. Fournet, M. Cadek, A. Drury, S. Hutzler, S. Roth and W. J. Blau, *J. Appl. Phys.*, 2001, **92**, 4024.
36 Z. Ounaies, C. Park, K. E. Wise, E. J. Siochi and J. S. Harrison, *Compos. Sci. Technol.*, 2003, **63**, 1637.
37 C. Park, Z. Ounaies, K. A. Watson, R. E. Crooks, J. Smith, Jr., S. E. Lowther, J. W. Connell, E. J. Siochi, J. S. Harrison and T. L. St. Clair, *Chem. Phys. Lett.*, 2002, **364**, 303.
38 J. Chen, A. M. Rao, S. Lyuksyutov, M. E. Itkis, M. A. Hamon, H. Hu, R. W. Cohn, P. C. Eklund, D. T. Colbert, R. E. Smalley and R. C. Haddon, *J. Phys. Chem. B*, 2001, **105**, 2525.
39 F. Patolsky, B. P. Timko, G. Zheng and C. M. Lieber, *MRS Bull.*, 2007, **32**, 142.
40 E. K. Hobbie, H. Wang, H. Kim, S. Lin-Gibson and E. A. Grulke, *Phys. Fluids*, 2003, **15**, 1196.
41 R. Bruinsma, W. M. Gelbart and A. Ben-Shaul, *J. Chem. Phys.*, 1992, **96**, 7710.
42 S. Kim and S. J. Karrila, *Microhydrodynamics: Principles and Selected Applications*, Butterworth–Heinemann, Boston, 1st edn, 1991, pp. 76–128.
43 Z. Wu, Z. Chen, X. Du, J. M. Logan, J. Sippel, M. Nikolou, K. Kamaras, J. R. Reynolds, D. B. Tanner, A. F. Hebard and A. G. Rinzler, *Science*, 2004, **305**, 1273.
44 M. Endo, H. Muramatsu, T. Hayashi, Y. A. Kim, M. Terrones and M. S. Dresselhaus, *Nature*, 2005, **433**, 476.
45 T. V. Sreekumar, T. Liu, S. Kumar, L. M. Ericson, R. H. Hauge and R. E. Smalley, *Chem. Mater.*, 2003, **15**, 175.
46 G. Yu, A. Cao and C. M. Lieber, unpublished results.
47 M. J. O'Connell, S. M. Bachilo, C. B. Huffman, V. C. Moore, M. S. Strano, E. H. Haroz, K. L. Rialon, P. J. Boul, W. H. Noon, C. Kittrell, J. Ma, R. H. Hauge, R. B. Weisman and R. E. Smalley, *Science*, 2002, **297**, 593.
48 F. Patolsky, G. Zheng and C. M. Lieber, *Anal. Chem.*, 2006, **78**, 4260.
49 E. Lueder, *Liquid Crystal Displays: Addressing Schemes and Electro-optical Effects*, Wiley & Sons, Chichester, England, 2001.
50 J.-H. Ahn, H.-S. Kim, K. J. Lee, S. Jeon, S. J. Kang, Y. Sun, R. G. Nuzzo and J. A. Rogers, *Science*, 2006, **314**, 1754.

